Synthesis T. Berking et al. THIEME OPEN ACCESS Feature

Kinetic or Thermodynamic Product? Case Studies on the Formation of Regioisomers of Tetraphenyladamantanes

Tim Berking
Wolfgang Frey
Clemens Richert*

Institute of Organic Chemistry, University of Stuttgart, Pfaffenwaldring 55, 70569 Stuttgart, Germany
lehrstuhl-2@oc.uni-stuttgart.de

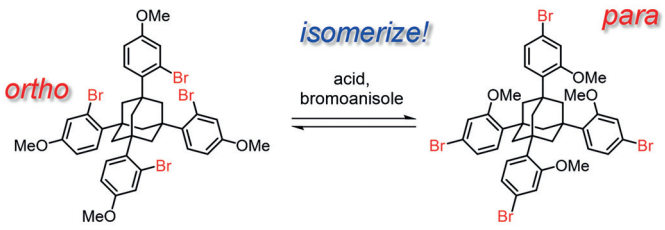

Received: 28.03.2023
Accepted after revision: 11.05.2023
Published online: 22.05.2023 (Accepted Manuscript), 19.06.2023 (Version of Record)
DOI: 10.1055/a-2097-0092; Art ID: SS-2023-03-0145-FA

Abstract Tetraaryladamantanes (TAAs) with alkoxyphenyl groups are interesting synthetic targets because they can act as crystallization chaperones for liquid compounds. Their carbon framework is set up by Friedel–Crafts alkylation, using adamantane-1,3,5,7-tetraol and anisole derivatives as starting materials. One successful chaperone is 1,3,5,7-tetrakis(2-bromo-4-methoxyphenyl)adamantane (TBro). This compound was initially considered the thermodynamic product of alkylation and its reaction towards strong Brønsted acid is reported. We now report that exposure of TBro to strong Brønsted acid leads to its regioisomer 1,3,5,7-tetrakis(4-bromo-2-methoxyphenyl)adamantane (iTBro) as the dominant product, obtained in a yield of 68%, far surpassing the 20% yield reported earlier for TBro. We also investigated the reactions of 3-iodo-, 3-chloro-, and 3-fluoroanisole to the corresponding TAAs and obtained yields of 66%, 26% and 52% for the main regioisomer. While 3-iodoanisole gave the same regioisomer as bromoanisole, 3-chloroanisole afforded complex mixtures and 3-fluoroanisole furnished 1,3,5,7-tetrakis(2-fluoro-4-methoxyphenyl)adamantane (TFM) in 52% yield as the main product. When mixtures of regioisomers were isomerized with an excess of triflic acid, the thermodynamic products were obtained in 76–91%. These results show how subtle effects govern the regioisomeric product distribution of aryladamantanes. They also help to make novel crystallization chaperones accessible in high yields.

Key words adamantane, alkylation, crystallization, Friedel–Crafts reactions, regioselectivity

Introduction

Adamantane is a highly symmetrical, rigid hydrocarbon that may be considered the smallest three-dimensional subunit of the diamond lattice. Substituted adamantanes are used to prepare cyclophanes,[1–4] to obtain materials for the storage and capture of small molecules from the liquid phase,[2] porous materials,[5,6] optical materials,[7,8] or as active pharmaceutical ingredients.[9,10] Further, adamantanes are interesting building blocks for erecting designed nanostructures[11–15] or hydrogen-bonded networks.[16–18] The synthesis of adamantanes has been explored in detail by Landa, Stetter, and colleagues.[19–23] These studies confirmed that the bridgehead carbon atoms can be derivatized by substitution reactions, including electrophilic substitution leading to phenyladamantanes.

Some tetraaryladamantane ethers have attracted interest because of their ability to include other molecules in their crystalline lattice.[24–32] Building on earlier work on diaryladamantanes[17] we recently showed that 1,3,5,7-tetrakis-(2,4-dimethoxyphenyl)adamantane (TDA), 1,3,5,7-tetrakis-(2,4-diethoxyadamantane (TEO), and 1,3,5,7-tetrakis(2-bromo-4-methoxyphenyl)adamantane (TBro) are able to act as crystalline hosts for liquid compounds. This property makes them useful as crystalline coats for hazardous or reactive compounds,[30] or reversible uptake of volatile organic compounds from the gas phase.[31] Further, either of these TAAs can be used as crystallization chaperones to determine the absolute configuration of small molecules that are liquids at room temperature.[32]

The tetraaryladamantanes mentioned above can be synthesized by a route adapted from the work of Stetter,[19–22] starting with four-fold bromination of adamantane in the presence of a strong Lewis acid. The halogenation is not accelerated by light irradiation, indicating that the reaction does not follow a radical, but rather an ionic mechanism.[20] This may be explained by the stability of the adamantyl carbenium ion, favored by the hydrocarbon framework.[33] While the first, second, and third halogenation occurs at ambient temperature, the fourth bromination requires reflux, though, indicating a loss of reactivity with higher functionalization. Studies on the mechanism of bromination of adamantane can be found in the literature.[34,35] After a two-step conversion to adamantane-1,3,5,7-tetraol (TOA), a Friedel–Crafts alkylation gives symmetrical tetraaryladamantanes. The alkylation requires strong Brønsted acids, like tosylic acid, and elevated temperatures. We observed that weaker acids or lower temperatures did not lead to

conversion of TOA, indicating a low reactivity of the adamantane species involved.

Perhaps the most interesting crystallization chaperone, co-crystallizing with analytes up to a molecular weight of 242 g/mol, is TBro.[28] Unfortunately, TBro is accessible in modest yields only, not exceeding 20% for the Friedel–Crafts alkylation step starting from TOA and bromoanisole. Unlike the aryl starting materials for TDA and TEO, bromoanisole **3** contains two different substituents on its phenyl ring, either of which is *ortho*/*para*-directing, so that regioisomers are likely to be formed in the alkylation step. When the synthesis of TBro was disclosed,[32] only the isolation of the symmetrical product with all four phenyl rings bearing *ortho*-bromo substitutuents was presented. It was likely that regioisomers with *para*-halo substituents were also formed (Figure 1, vide infra).

Attempts to optimize the synthesis of TBro led to the question what the most stable regioisomers of the alkylation is, as this should be the predominant product for reactions under thermodynamic control. We initially assumed that this was TBro itself, and performed numerous reactions aimed at establishing the equilibrium in alkylation before decomposition of the anisole dominated the reaction processes. These attempts were unsuccessful. Here we report the formation and isolation of the regioisomer tetrakis(4-bromo-2-methoxyphenyl)adamantane (iTBro) as the main product of the Friedel–Crafts reaction under the control of a strong Brønsted acid, indicating that this is the true thermodynamic product of the Friedel–Crafts alkylation of TOA. We also extended our study to reactions with the other three halogens, starting from 3-fluoro-, 3-chloro-, or 3-iodoanisole. Besides the preferred regioisomers of the

Biographical Sketches

Tim Berking was born in Essen, Germany in 1995. He studied chemistry at the University of Wuppertal. In 2019, he investigated gold-catalyzed cyclizations during a research internship at the Australian National University in Canberra in the group of M. Banwell and got his Master's degree in 2020 working on selective inhibitors of cytochrome P450 monooxygenases under the supervision of S. Kirsch. After a 3-month internship at Bayer AG in Wuppertal, Germany, he joined the group of Prof. Clemens Richert as a graduate student in 2021, working on tetraaryladamantanes as crystallization chaperones.

Wolfgang Frey was born in Stuttgart, Germany in 1957. He studied chemistry at the University of Stuttgart. He got his diploma degree in 1985 in the group of John Stezowski working on crystallographic investigations of inverse charge-transfer complexes. In 1991, he obtained his Ph.D. in chemistry for structural investigations on cytostatically active acridine derivatives with crystallographic and semiempirical methods in the group of John Stezowski in Stuttgart. Since 1996 he is the head of the X-ray division of the Institute of Organic Chemistry at the University of Stuttgart.

Clemens Richert was born in Münster, Germany in 1965. He studied chemistry at the Universities of Münster (Vordiplom 1987) and Cologne (Diplom1990). For his diploma thesis he synthesized novel porphycene photosensitizers. He obtained a Ph.D. in human biology from the Ludwigs-Maximilians University of Munich in 1993, working in the Institute for Surgical Research. In 1994, he obtained a Ph.D. in chemistry from the ETH Zurich for work on non-ionic RNA analogues. In 1995, he became assistant professor of chemistry at Tufts University in the USA. From 2000 until 2002 he was associate professor at the University of Konstanz. In 2002, he moved to the University of Karlsruhe (TH), where he was Professor of Chemistry until 2008, when he moved to his current position as Professor of Chemistry at the University of Stuttgart.

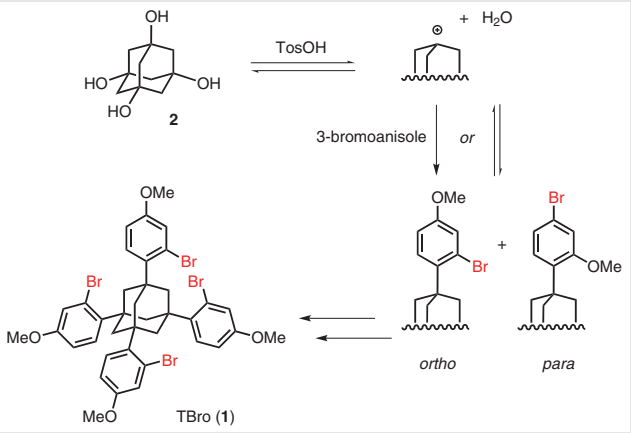

Scheme 1 Synthesis of TBro and the issue of regioselectivity of the alkylation step, depending on the reversibility of this step.

alkylation of those haloanisoles, our report also includes two X-ray crystal structures of iTBro, with or without inclusion of a solvent as guest in its crystal lattice.

Results and Discussion

We started our optimization study on the synthesis of TBro (**1**), an established crystallization chaperone,[32] by varying the acid catalyst and the temperature of the Friedel–Crafts alkylation. When we continued to obtain TBro in low and variable yields, the crudes were analyzed in more detail. We suspected that either of the two *ortho*/*para*-positions of 3-bromoanisole (**3**) reacted with the carbenium ion intermediates formed from TOA (Scheme 1). Five different regioisomeric tetraaryladamantanes may form in this reaction, as illustrated in Scheme 2. These range from the symmetrical TAAs TBro and iTBro (**4**) to the partially isomerized counterparts **5**–**7**.

To facilitate visual recognition of the isomeric nature of each species, rhombi with four colored fields representing the aryl arms are defined in Scheme 2 and were used as symbols to assign peaks in spectra. The isomer distribution was determined by ^{1}H NMR spectroscopy. Figure 1 shows representative spectra for a mixture of regioisomers and one of the symmetrical products (iTBro).

Selected results of the optimization study are compiled in Table 1. First, we increased the reaction temperature to 140 °C to favor isomerization to the thermodynamically most stable product. Instead of increasing the yield of TBro, the higher temperature seemed to favor the other regioisomers. In addition, it was observed that reducing the reaction time to 16 hours increased the overall yield of the sum of the regioisomeric tetraaryladamantane products. We suspected that the decreased yield after longer reaction times was due to ether cleavage under the harsh acidic con-

Table 1 Distribution of TBro Isomers[a]

Entry	Time (h)	Acid (equiv)	TBro (%)	**5** (%)	**6** (%)	**7** (%)	iTBro (%)
1	48	1	7	17	13	n.i.	<1
2	16	1	10	27	16	8	<1
3	2	10	<1	<1	<1	17[b]	68[b]

[a] The isomers are obtained by the alkylation of 3-bromoanisole with TOA in the presence of tosylic acid under different reaction times and catalyst concentrations at 140 °C. n.i.: Not isolated.
[b] Product distribution determined by ^{1}H NMR spectroscopy

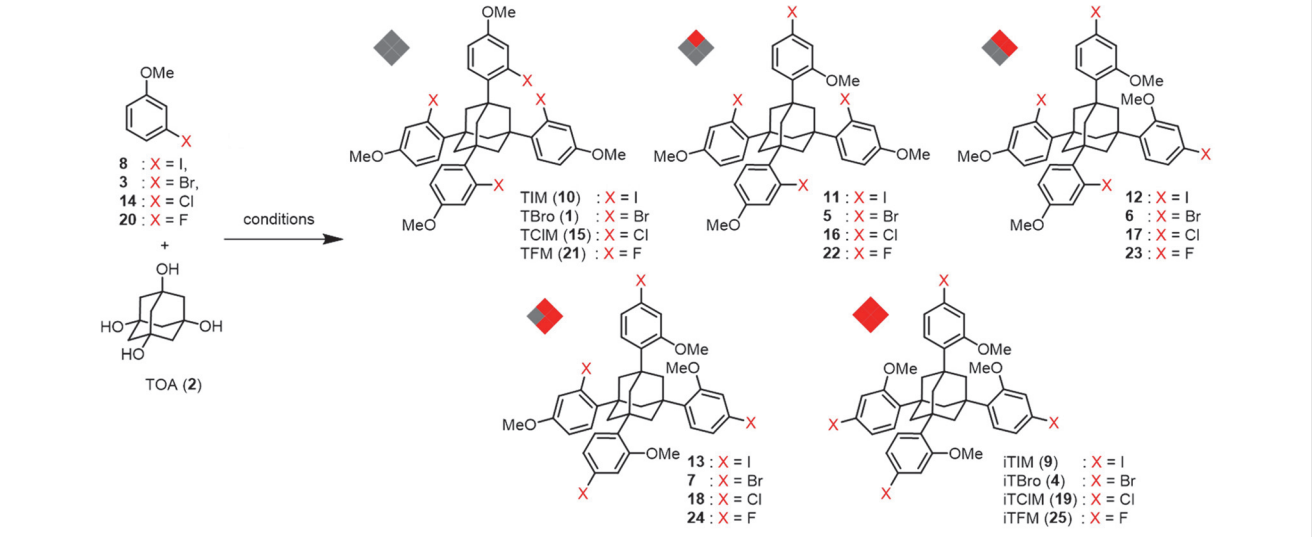

Scheme 2 Acid-catalyzed Friedel–Crafts reaction of 3-haloanisoles and adamantane tetraol TOA to five different regioisomeric products. Colored rhombi represent isomers, with grey for *ortho*-methoxy and red for *ortho*-halosubstituted phenyl rings.

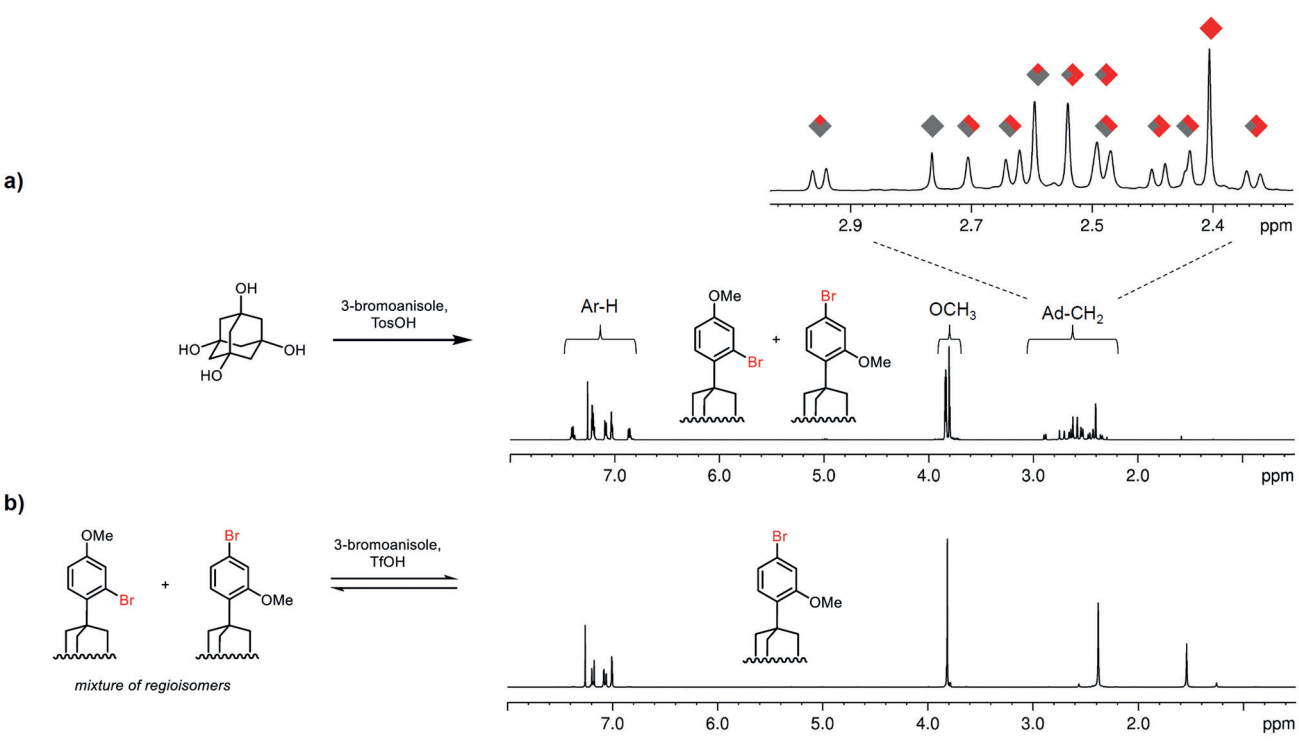

Figure 1 Representative spectra from NMR analysis of the products of the Friedel–Crafts alkylation of Scheme 2. a) ^{1}H NMR spectrum (700 MHz) of a mixture of TBro regioisomers, obtained in a reaction employing 1 equiv of tosylic acid for 6 d at 140 °C, with an expansion of the aliphatic region showing the assignment of peaks to the regioisomers. For the definition of symbols of the assignment, see Scheme 2. b) ^{1}H NMR spectrum (400 MHz) of the crude product obtained when employing 10 equiv of triflic acid and the mixture of TBro isomers in 80 equiv of 3-bromoanisole for 65 h. Here, iTBro is the predominant product.

ditions. The formation of methyl tosylate, the side product expected for cleavage of the methyl ethers, could indeed be detected. We also suspected that the harsh reactions conditions favored thermal decomposition over time. To reduce this, the catalyst 'loading' was increased to 10 equivalents (Table 1, entry 3). Interestingly, we now observed **7** and iTBro as the main products. Higher temperatures, longer or shorter reaction times or more acid catalyst led to lower yields of iTBro, though.

The screening of reaction conditions did not give a higher yield for TBro than the one recently published.[32] The most reproducible result was obtained with one equivalent tosylic acid and a reaction temperature of 140 °C. Under those conditions, 10% of TBro was isolated after 16 hours. So, the optimization study gave two different acid concentration/reaction time optima for the two fully symmetrical alkylation products TBro/iTBro. The optimum for iTBro is referred to as 'short', and the one for TBro as 'long' below.

We then ran the Friedel–Crafts alkylations under the conditions of either of the two optima for the other 3-haloanisoles (Fl, Cl, I). The results are compiled in Table 2. Iodoanisole **8** gave iTIM (**9**) as the predominant product under conditions of the short protocol, resulting in an isolated yield of 66%, but a yield of just 5% for the long reaction time (Table 2, entries 1 und 2). No TIM (**10**), with all iodo substituents in the *ortho*-position of phenyl groups was detectable, and the balance of isolated TAAs obtained with the long protocol was made up of regioisomers of lower symmetry (**11**–**13**) and iTIM (**9**). The lighter haloanisole, 3-chlo-

Table 2 Yields of Fully Symmetric Products for the Tosylic Acid Induced Friedel–Crafts Alkylations of TOA[a]

Entry	Halogen	Conditions	Product	Yield [%]	Product	Yield [%]
1	I	short	TIM	<1	iTIM	66
2	I	long	TIM	<1	iTIM	5
3	Br	short	TBro	<1	iTBro	68[b]
4	Br	long	TBro	10	iTBro	<1
5	Cl	short	TClM	<1	iTClM	26[b]
6	Cl	long	TClM	14[c]	iTClM	<1
7	F	short	TFM	52	iTFM	<1
8	F	long	TFM	11	iTFM	<1

[a] The reaction was conducted with different haloanisoles and a 2 h reaction time with 10 equiv acid (short) or 16 h reaction time with 1 equiv acid (long). Reactions were performed at 140 °C.
[b] Determined by ^{1}H NMR spectroscopy.
[c] Impure fraction, containing residual regioisomers.

roanisole (**14**), gave complex mixtures of regioisomers **15**–**19** under both conditions (entries 5 and 6), indicating that there is little kinetic or thermodynamic preference for either *ortho*- or *para*-halogen products.

In the case of 3-fluoroanisole (**20**), the balance of factors determining regioselectivity was found to be tipped to the other side. Here, the fully symmetrical *ortho*-halo isomer TFM (**21**) was the preferred product using the 'short' reaction conditions, resulting in an isolated yield of 52%, When the long reaction time and lower acid concentration was employed, a broader range of regioisomeric products (**21**–**24**) was found, containing just 11% of TFM. Neither of the reaction conditions gave detectable quantities of the fully symmetrical counterpart iTFM (**25**) (Table 2, entries 7 and 8).

The results from the optimization study did not give a conclusive answer which of the two regioisomers (TBro or iTBro) is the thermodynamically more stable product. A long reaction time should help to achieve equilibrium, and so should a high concentration of catalyst. To shed more light on this issue, we attempted to induce isomerization in regioisomeric mixtures isolated in TAA-forming reactions that did not yield a single isomer. If Friedel–Crafts alkylation was reversible, which seemed likely, given that the carbenium ions of the adamantane framework are exceptionally stable, a change in isomeric composition should result under these conditions. Again, the first experiments involved the regioisomers with bromoanisole substituents. Monitoring by TLC indicated conversion of isomeric mixtures from the TBro-forming reaction mixture when this separate isomerization step was induced with one equivalent of tosylic acid at 140 °C in the presence of 80 equivalents of bromoanisole as solvent and reaction partner, confirming the reversibility of alkylation. As the reaction progressed, there was a shift in product distribution toward iTBro, suggesting that this is the true thermodynamically more stable product.

Since tosylic acid gave slow isomerization, with incomplete conversion after 1 week at 140 °C, we searched for other catalysts. It was found that triflic acid catalyzes significantly faster isomerization. When exposing a mixture of pre-synthesized TBro isomers to an excess of this acid in 3-bromoanisole as solvent, iTBro was produced as the predominant product within 65 hours, with only traces of isomer **7** remaining, resulting in an isolated yield of the fully symmetrical product of 91% from this mixture (Table 3, entry 1). The NMR spectrum of the crude product, obtained at the end of the isomerization with triflic acid, is shown in Figure 1b.

A similar result was obtained when an isomeric mixture of TAAs resulting from the alkylation of 3-chloroanisole was subjected to isomerization with triflic acid at room temperature. Using 3-chloroanisole as solvent, a product mixture formed that contained 76% of iTClM, as determined by NMR (Table 3, entry 2). No attempt to purify the fully symmetrical TAA was made, though, due to the low solubility of iTClM. Under the same conditions, the regioisomeric mixture obtained in the Friedel–Crafts reaction with 3-fluoroanisole and one equivalent of tosylic acid (Table 2, entry 8) gave TFM as the predominant species in the isomerization, resulting in 87% isolated yield. Isomerization of TIM regioisomers was not attempted, as pure iTIM was already obtained with the 'short' protocol in the initial alkylation reaction (Table 2).

Table 3 Products of the Isomerization of TAA Mixtures[a]

Entry	Halogen	Product	Yield (%)	Product	Yield (%)
1	Br	TBro	<1	iTBro	91
2	Cl	TClM	<1	iTClM	76[b]
3	F	TFM	87	iTFM	<1

[a] The reaction was conducted with 10 equiv of triflic acid and 80 equiv of the respective haloanisole for 65 h at 25 °C.
[b] Isomer distribution determined by ^{1}H NMR spectroscopy.

Some exploratory crystallography experiments were then performed for the now well accessible tetraaryladamantane iTBro. These experiments were hampered by the much lower solubility of this TAA, as compared to TBro or the halogen-free sister chaperones TDA and TEO, in the liquids tested. Still, the initial screen readily produced crystals suitable for X-ray diffractometry (Figure 2).[36] A solvate-free form was obtained by thermally crystallizing from acetone. When a mixture of glacial acetic acid and dichloromethane (10:1) was used as solvent, crystals of a solvate form were found that is shown in Figure 2c/d. Here, the halogenated solvent was incorporated at a molar ratio of 3:2 (solvent/TAA), and two types of CH_2Cl_2 guest molecules were found in the crystal lattice. One type is well packed, resulting in a well-resolved molecular structure, but the one in the other crystal site showed partially disordered dichloromethane molecules. Also, only one of the two solvents employed (CH_2Cl_2/AcOH) was encapsulated, indicating selectivity in the co-crystallization process.

These results are interesting on several levels. On the level of chemical reactivity and thermodynamic stability, the identification of the *para*-halogen-substituted TAAs as predominant products of alkylations with bromo- and iodoanisole, when a large excess of tosylic acid or a very strong Brønsted acid (TfOH) are used, indicates that these are the thermodynamically most stable products, and that TBro, isolated as the only pure product in modest yield in earlier work, is a kinetic product. For chlorine as halogen, stability and reactivity of the different isomers appears to be so similar that it is difficult to obtain pure, fully symmetrical products for either of the regiosiomeric orientations (*ortho* or *para*). For fluoroanisole, there is a clear preference for the *ortho*-halo TAA, most probably because of steric and electronic reasons. The same can be said of the forces that

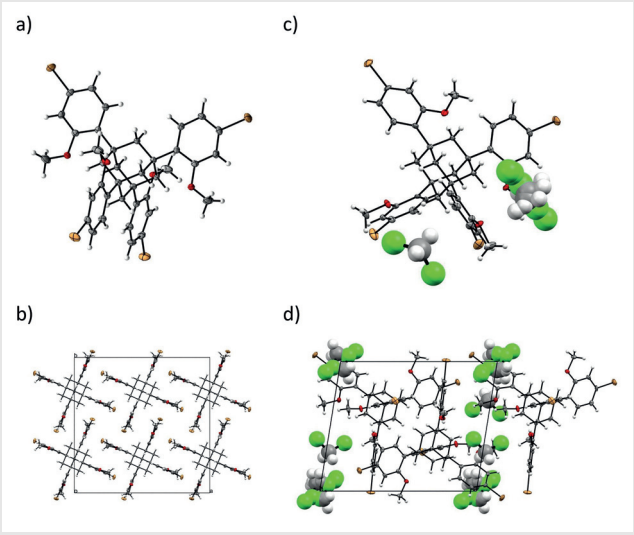

Figure 2 Structures of iTBro in two crystalline forms, as determined by X-ray crystallography. a) Structure of the TAA in the solvate-free form, obtained by crystallizing from acetone, and b) asymmetric unit of the same. c) View of the TAA and two of the guest molecules encapsulated in the crystal lattice when crystallizing from CH_2Cl_2/glacial AcOH (1:10). We note that one solvent molecule is well ordered, while the other one is partially disordered. d) Crystal packing in the solvate form with CH_2Cl_2. Shown are ORTEP plots at 50% probability. For the solvate form, van der Waals radii for the guest molecules were set to 40%. Color code: grey = carbon, white = hydrogen, red = oxygen, ochre = bromine, and green = chlorine.[36]

favor the iodo derivative iTIM over TIM, with an even stronger steric effect when the bulky halogen is proximal to the adamantane core.

On the level of catalysis, it is interesting to see how different tosylic and triflic acid perform, depending on whether the initial Friedel–Crafts alkylation or a subsequent isomerization of pre-formed TAAs is concerned. For the former reaction, tosylic acid remains the catalyst of choice (many other Brønsted and Lewis acids have been tested by us unsuccessfully), and elevated temperatures are required, probably at least in part because the water formed in the reaction must be removed from the equilibrium. The isomerization, which most probably is an intermolecular process involving dearylation and rearylation, works best with triflic acid at 25 °C, though. One possible explanation for this is that the stronger acid and its harder conjugate base are less prone to induce ether cleavage, a side reaction that limits yields in the initial alkylation step and reduces the concentration of the free acid. Further, the stronger acid is more likely to produce a Wheland intermediate, and the lower temperature then probably shifts the equilibrium from free carbenium ions and anisoles to the bound form on entropic grounds, favoring isomerization. Independent of such considerations, it is important to know that retro-Friedel–Crafts reactions can be induced under such mild conditions, and that the initial alkylation is low-yielding when performed with triflic acid.

On the level of the applications as crystallization chaperone, the results are also interesting, as iTBro and iTIM are behaving quite differently from the established TAA chaperones TBro, TDA, and TEO. Either of the *para*-halo isomers are poorly soluble in common organic solvents, making it challenging to use them in thermal co-crystallization with analytes that do not have good solvent properties. Further, iTBro gives a stable solvate with dichloromethane (Figure 2), that is, a solvent that leads to unstable solvate crystals for TDA and TEO,[25] due to loss of encapsulated solvent upon exposure to air. In the case of iTBro, the crystals are stable and the halogenated solvent is well ordered at one of its positions in the crystal lattice. Still, the low solubility, most probably induced by a network of strong packing forces involving the halogens exposed at the distal tips of the aryl arms, makes these compounds unlikely candidates for encapsulation of a wide range of different guest molecules.[37]

On the level of synthetic applications, iTIM and iTBro are interesting building blocks, as they offer access to cross coupling products extending the aryl arms in Pd-catalyzed synthetic transformations.[38] Both should be suitable for a range of different reaction partners and conditions, so that structurally interesting, large and rigid target molecules[39] may be prepared based on these TAAs that are now accessible in high yield and purity.

In summary, we have identified what we believe to be the thermodynamic products of the four-fold Friedel–Crafts alkylation of adamantane-1,3,5,7-tetraol and 3-iodo-, 3-bromo-, 3-chloro-, and 3-fluoroanisole. For the heavy halogens, the *para*-halo TAAs are the predominant products of equilibria induced by treatment with the strong Brønsted acid triflic acid, whereas fluoroanisole gives predominantly the regioisomeric *ortho*-halogen product under conditions that allow for establishing isomerization equilibria. The resulting 1,3,5,7-tetrakis(2-fluoro-4-methoxyphenyl)adamantane will be studied further as a potential chaperone for the encapsulation of compounds that do not crystallize by themselves.

Adamantane, Br_2, $AlCl_3$, 3-iodoanisole, 3-chloroanisole, 3-fluoroanisole, and tosylic acid (TosOH) were purchased from Sigma-Aldrich (Darmstadt, Germany) and were used without further purification. The 3-bromoanisole, Ag_2SO_4, and CF_3SO_3H were from Fluorochem (Dublin, Ireland) and were also used without further purification. The synthesis of adamantane-1,3,5,7-tetraol (TOA) followed published protocols.[22,25] Silica gel 60 (0.040–0.063 mm) particle size (Macherey-Nagel, Düren, Germany) was used for column chromatography, and TLC was conducted on pre-coated TLC sheets ALUGRAM from Macherey-Nagel, with visualization by UV (254 nm) and staining with phosphomolybdic acid reagent. NMR Spectra were recorded on Bruker 300 MHz, 400 MHz, or 700 MHz spectrometer. Chemical shifts (δ) are reported in ppm, coupling constants (*J*) are in hertz (Hz). High-resolu-

tion mass spectra (EI or ESI) were measured on a Bruker micrOTOF-Q-spectrometer. Diffraction data were collected on a KAPPA APEXII DUO diffractometer from Bruker AXS at 140 K using MoKα (λ = 0.71073 Å) or CuKα (λ = 1.54178 Å). Cell refinement and data reduction were performed with the SAINT program package and absorption correction with SADBAS3. Structures were solved by direct methods using SHELXL97, including isotropic refinement by least-squares methods. The positions of the hydrogens were calculated geometrically with riding models. The crystallographic data graphics were generated with Mercury v3.8.0.[36]

Friedel–Crafts Alkylation with Long Reaction Time; General Protocol A

The following protocol is for the preparation of 1,3,5,7-tetrakis(2-bromo-4-methoxyphenyl)adamantane (TBro, **1**) and its isomers **5**–**7** and is representative. In a 50 mL round-bottom flask, a mixture of adamantane-1,3,5,7-tetraol (TOA, **2**; 100 mg, 500 µmol), tosylic acid (95 mg, 500 µmol, 1 equiv), and 3-bromoanisole (5.1 mL, 40.0 mmol, 80 equiv) was heated to 140 °C (bath temperature, preheated) for 16 h. The reaction mixture was diluted with CH_2Cl_2 (50 mL) and washed with sat. aq $NaHCO_3$ (30 mL). The aqueous solution was extracted with CH_2Cl_2 (50 mL), and the combined organic phases were washed with brine (30 mL), dried (Na_2SO_4), and concentrated under reduced pressure. The excess 3-bromoanisole was removed under vacuum at 7 mbar and 100 °C (bath temperature). The resulting brownish residue was taken up in CH_2Cl_2 (20 mL) and precipitated through addition of MeOH (50 mL). Precipitation was allowed to continue by cooling to 0 °C for 1 h. The precipitate was isolated by filtration, and the precipitation was repeated two more times, yielding a colorless solid, which was purified by column chromatography with petroleum ether (PE)/CH_2Cl_2 (6:4 to 4:6, v/v) as eluent.

Friedel–Crafts Alkylation with Short Reaction Time; General Protocol B

The following protocol is for the preparation of iTBro (**4**) and its isomer **7** and is representative. The protocol with short reaction time followed General Protocol A, except that 10 equiv of tosylic acid (950 mg, 5.00 mmol) instead of 1 equiv were used with a reaction time of 2 h instead of 16 h. The precipitation yielded 374 mg (427 mmol, 85%) of a mixture of **7** and iTBro (**4**) as a colorless solid, which was not further purified due to low solubility.

Isomerization of Tetraaryladamantanes; General Protocol C

This protocol is for the isomerization of TBro and its isomers and is representative. In an oven-dried round-bottom flask, a mixture of regioisomers of TBro **1** and **4**–**7** (6.36 g, 7.25 mmol), TfOH (6.4 mL, 72.5 mmol, 10 equiv), and 3-bromoanisole (73.5 mL, 580 mmol, 80 equiv) was stirred under a N_2 atmosphere at 25 °C for 65 h. The reaction mixture was then poured onto sat. aq $NaHCO_3$ (400 mL) at 0 °C, and the resulting mixture stirred for 1 h. The precipitate was collected by filtration, washed with H_2O (100 mL) and CH_2Cl_2 (50 mL) and dried by exposing to air for 1 h, giving 5.34 g (6.09 mmol, 84%) of iTBro (**4**) as a colorless solid. To obtain additional product, the filtrate was diluted with CH_2Cl_2 (100 mL), and the aqueous phase was extracted with CH_2Cl_2 (2 × 100 mL). The combined organic phases were washed with brine (100 mL), dried (Na_2SO_4), filtered, and the solvent was removed under reduced pressure. The resulting residue was triturated with CH_2Cl_2 (20 mL), followed by decanting and filtration. The trituration was repeated once. The remaining solid was dried on air for 1 h, giving additional 466 mg (531 µmol, 7%) of iTBro (**4**) as a colorless solid. In total 5.81 g (6.63 mmol, 91%) of iTBro (**4**) was isolated.

1,3,5,7-Tetrakis(2-bromo-4-methoxyphenyl)adamantane (TBro, 1) and its Regioisomers 4–7

A synthesis according to General Protocol A yielded 44 mg (51 µmol, 10%) of TBro (**1**), 120 mg (137 µmol, 27%) of **5**, 74 mg (84 µmol, 17%) of **6** and 28 mg (32 µmol, 6%) of **7** as colorless solids.

A synthetic run using General Protocol B, gave a mixture of **7** and iTBro (**4**) mentioned at the end of the general protocol. An isomer distribution (**7**:iTBro) of 1:3.95 was determined by ^{1}H NMR spectroscopy) of the solid obtained, indicating that this product consisted of 76 mg (87 µmol, 18%) **7**, and 298 mg (340 µmol, 68%) of iTBro (**4**).

The yield of a synthesis according to General Protocol C is given above.

1,3,5,7-Tetrakis(2-bromo-4-methoxyphenyl)adamantane (TBro, 1)

R_f = 0.15 (PE/CH_2Cl_2 1:1, v/v).

^{1}H NMR (400 MHz, $CDCl_3$): δ = 7.44 (d, *J* = 8.9 Hz, 4 H), 7.20 (d, *J* = 2.7 Hz, 4 H), 6.86 (dd, *J* = 8.9, 2.8 Hz, 4 H), 3.79 (s, 12 H), 2.74 (s, 12 H).

^{13}C NMR (101 MHz, $CDCl_3$): δ = 159.2, 138.3, 129.0, 122.5, 121.8, 113.1, 55.2, 42.2, 41.5, 40.7.

1-(4-Bromo-2-methoxyphenyl)-3,5,7-tris(2-bromo-4-methoxyphenyl)adamantane (5)

R_f = 0.24 (PE/CH_2Cl_2 1:1, v/v).

^{1}H NMR (400 MHz, $CDCl_3$): δ = 7.39 (d, *J* = 8.9 Hz, 3 H), 7.20–7.18 (m, 4 H), 7.06 (dd, *J* = 8.3, 1.9 Hz, 1 H), 7.01 (d, *J* = 1.9 Hz, 1 H), 6.84 (dd, *J* = 8.9, 2.8 Hz, 3 H), 3.83 (s, 3 H), 3.79 (s, 9 H), 2.87 (d, *J* = 11.8 Hz, 3 H), 2.60 (s, 6 H), 2.52 (d, *J* = 12.0 Hz, 3 H).

^{13}C NMR (101 MHz, $CDCl_3$): δ = 159.3, 158.0, 138.4, 128.9, 128.0, 123.4, 122.4, 121.6, 120.6, 114.2, 113.0, 55.5, 42.1, 40.9, 40.5, 39.6.

HRMS (EI): *m*/*z* calcd for $C_{38}H_{36}{}^{79}Br_2{}^{81}Br_2O_4$: 875.9306; found: 875.9301.

1,3-Bis(2-bromo-4-methoxyphenyl)-5,7-bis(4-bromo-2-methoxyphenyl)adamantane (6)

R_f = 0.36 (PE/CH_2Cl_2 1:1, v/v).

^{1}H NMR (400 MHz, $CDCl_3$): δ = 7.40 (d, *J* = 8.9 Hz, 2 H), 7.22–7.20 (m, 4 H), 7.08 (d, *J* = 8.4 Hz, 2 H), 7.02 (s, 2 H), 6.85 (dd, *J* = 8.8, 2.7 Hz, 2 H), 3.83 (s, 6 H), 3.79 (s, 6 H), 2.69 (s, 2 H), 2.63 (d, *J* = 12.0 Hz, 4 H), 2.52 (d, *J* = 11.9 Hz, 4 H), 2.41 (s, 2 H).

^{13}C NMR (101 MHz, $CDCl_3$): δ = 159.3, 158.0, 138.6, 136.2, 128.8, 128.0, 123.5, 122.4, 121.6, 120.6, 115.0, 113.0, 55.49, 55.46, 42.5, 41.5, 41.3, 40.4.

HRMS (EI): *m*/*z* calcd for $C_{38}H_{36}{}^{79}Br_2{}^{81}Br_2O_4$: 875.9306; found: 875.9299.

1-(2-Bromo-4-methoxyphenyl)-3,5,7-tris(4-bromo-2-methoxyphenyl)adamantane (7)

R_f = 0.51 (PE/CH_2Cl_2 1:1, v/v).

^{1}H NMR (400 MHz, $CDCl_3$): δ = 7.38 (d, *J* = 8.9 Hz, 1 H), 7.21–7.19 (m, 4 H), 7.07 (d, *J* = 8.4 Hz, 3 H), 7.01 (s, 3 H), 6.84 (dd, *J* = 8.9, 2.6 Hz, 1 H), 3.82 (s, 9 H), 3.78 (s, 3 H), 2.56 (s, 6 H), 2.45 (d, *J* = 11.7 Hz, 3 H), 2.33 (d, *J* = 11.9 Hz, 3 H).

^{13}C NMR (101 MHz, $CDCl_3$): δ = 159.5, 158.1, 138.9, 136.6, 134.3, 129.0, 128.2, 123.6, 122.6, 121.7, 120.7, 115.2, 113.1, 55.6, 55.5, 41.9, 40.3, 39.6.

HRMS (EI): *m*/*z* calcd for $C_{38}H_{36}{}^{79}Br_2{}^{81}Br_2O_4$: 875.9306; found: 875.9301.

1,3,5,7-Tetrakis(4-bromo-2-methoxyphenyl)adamantane (iTBro, 4)

R_f = 0.85 (PE/CH_2Cl_2 1:1, v/v).

^{1}H NMR (400 MHz, $CDCl_3$): δ = 7.19 (d, *J* = 8.4 Hz, 4 H), 7.07 (dd, *J* = 8.3, 1.3 Hz, 4 H), 7.01 (d, *J* = 1.3 Hz, 4 H), 3.82 (s, 12 H), 2.38 (s, 12 H).

^{13}C NMR (101 MHz, $CDCl_3$): δ = 159.5, 136.8, 128.2, 123.6, 120.6, 115.3, 55.5, 42.0, 39.5.

HRMS (EI): *m*/*z* calcd for $C_{38}H_{36}{}^{79}Br_2{}^{81}Br_2O_4$: 875.9306; found: 875.9302.

1,3,5,7-Tetrakis(4-iodo-2-methoxyphenyl)adamantane (iTIM) and its Regioisomers 11–13)

Synthesis according to General Protocol A, using 3-iodoanisole (4.8 mL, 40.3 mmol, 80 equiv) and purification by column chromatography using a gradient of CH_2Cl_2 in PE (PE/CH_2Cl_2 6:4 to 4:6, v/v), yielded 54 mg (51 µmol, 10%) of **11**, 143 mg (134 µmol, 27%) of **12**, (80 µmol, 21%) of **13**, and 25 mg (23 µmol, 5%) of iTIM (**9**) as colorless solids.

General Protocol B, starting from TOA (292 mg, 1.46 mmol), tosylic acid (2.78 g, 14.6 mmol, 10 equiv) and 3-iodoanisole (13.9 mL, 117 mmol, 80 equiv), followed by recrystallization from toluene, yielded 1.03 g (968 µmol, 66%) of iTIM (**9**) as a colorless solid.

1-(4-Iodo-2-methoxyphenyl)-3,5,7-tris(2-iodo-4-methoxyphenyl)adamantane (11)

R_f = 0.21 (PE/CH_2Cl_2 1:1, v/v).

^{1}H NMR (400 MHz, $CDCl_3$): δ = 7.61 (d, *J* = 2.8 Hz, 2 H), 7.37 (d, *J* = 8.9 Hz, 3 H), 7.30 (dd, *J* = 8.3, 1.6 Hz, 2 H), 7.18 (d, *J* = 1.6 Hz, 2 H), 7.07 (d, *J* = 8.4 Hz, 3 H), 6.91 (dd, *J* = 8.8, 2.8 Hz, 1 H), 3.83 (s, 3 H), 3.79 (s, 9 H), 3.07 (d, *J* = 11.8 Hz, 3 H), 2.62 (s, 6 H), 2.42 (d, *J* = 11.5 Hz, 3 H).

^{13}C NMR (101 MHz, $CDCl_3$): δ = 159.2, 157.7, 140.2, 136.7, 129.8, 129.7, 128.4, 128.3, 120.6, 113.5, 94.2, 92.0, 55.8, 55.5, 42.2, 40.6, 40.4, 39.9.

HRMS (EI): *m*/*z* calcd for $C_{38}H_{36}I_4O_4$: 1063.8787; found: 1063.8795.

1,3-Bis(2-iodo-4-methoxyphenyl)-5,7-bis(4-iodo-2-methoxyphenyl)adamantane (12)

R_f = 0.37 (PE/CH_2Cl_2 1:1, v/v).

^{1}H NMR (400 MHz, $CDCl_3$): δ = 7.61 (d, *J* = 2.8 Hz, 2 H), 6.36 (d, *J* = 8.9 Hz, 2 H), 7.29 (dd, *J* = 8.2, 1.7 Hz, 2 H), 7.18 (d, *J* = 1.6 Hz, 2 H), 7.07 (d, *J* = 8.3 Hz, 2 H), 6.91 (dd, *J* = 9.0, 2.8 Hz, 2 H), 3.82 (s, 6 H), 3.78 (s, 6 H), 2.77–2.72 (m, 6 H), 2.42–2.39 (m, 6 H).

^{13}C NMR (101 MHz, $CDCl_3$): δ = 159.2, 157.6, 140.3, 137.0, 129.8, 129.7, 128.4, 128.3, 120.7, 113.5, 94.2, 91.9, 55.6, 55.4, 43.0, 41.3, 40.6, 40.3, 39.7.

HRMS (EI): *m*/*z* calcd for $C_{38}H_{36}I_4O_4$: 1063.8787; found: 1063.8786.

1-(2-Iodo-4-methoxyphenyl)-3,5,7-tris(4-iodo-2-methoxyphenyl)adamantane (13)

R_f = 0.57 (PE/CH_2Cl_2 1:1, v/v).

^{1}H NMR (400 MHz, $CDCl_3$): δ = 7.60 (d, *J* = 2.8 Hz, 1 H), 7.33 (d, *J* = 8.9 Hz, 1 H), 7.29 (dd, *J* = 8.2, 1.6 Hz, 3 H), 7.17 (d, *J* = 1.7 Hz, 3 H), 7.05 (d, *J* = 8.3 Hz, 3 H), 6.88 (dd, *J* = 8.9, 2.8 Hz, 1 H), 3.81 (s, 9 H), 3.77 (s, 3 H), 2.56 (s, 6 H), 2.38 (s, 6 H).

^{13}C NMR (101 MHz, $CDCl_3$): δ = 159.2, 157.6, 140.5, 137.2, 129.8, 129.6, 128.4, 128.3, 120.8, 113.4, 94.1, 91.8, 55.5, 55.4, 41.8, 41.3, 40.1, 39.5.

HRMS (EI): *m*/*z* calcd for $C_{38}H_{36}I_4O_4$: 1063.8787; found: 1063.8787.

1,3,5,7-Tetrakis(4-iodo-2-methoxyphenyl)adamantane (iTIM, 9)

R_f = 0.64 (PE/CH_2Cl_2 7:3, v/v).

^{1}H NMR (400 MHz, $CDCl_3$): δ = 7.28 (dd, *J* = 8.3, 1.7 Hz, 4 H), 7.16 (d, *J* = 1.7 Hz, 4 H), 7.03 (d, *J* = 8.3 Hz, 4 H), 3.79 (s, 12 H), 2.36 (s, 12 H).

^{13}C NMR (101 MHz, $CDCl_3$): δ = 159.2, 137.4, 129.7, 128.4, 120.8, 91.7, 55.3, 41.6, 39.3.

HRMS (ESI): *m*/*z* calcd for $C_{38}H_{36}I_4O_4Na$: 1086.8685; found: 1086.8675.

1,3,5,7-Tetrakis(2-chloro-4-methoxyphenyl)adamantane (TClM, 15) and its Regioisomers 16–18

Synthesis according to General Protocol A, using 3-chloroanisole (4.9 mL, 40.0 mmol, 80 equiv) and chromatography with PE/CH_2Cl_2 6:4 to 4:6 (v/v) as eluent yielded 50 mg (72 µmol, 14%) of TClM (**15**) as a slightly impure fraction, 68 mg (97 µmol, 19%) of **16**, 57 mg (82 µmol, 16%) of **17**, and 13 mg (19 µmol, 4%) of **18** as colorless solids.

General Protocol B with TOA (200 mg, 1.00 mmol), tosylic acid (1.90 g, 10.0 mmol, 10 equiv), and 3-chloroanisole (9.8 mL, 80.0 mmol, 80 equiv), followed by precipitation by addition of MeOH to a solution in CH_2Cl_2 gave 465 mg (674 µmol, 67%) of a mixture of regioisomers. ^{1}H NMR spectroscopy indicated that this mixture consisted of 58 mg (83 µmol, 8%) of **17**, 226 mg (324 µmol, 32%) **18**, and 181 mg (259 µmol, 26%) of iTClM.

The isomerization of the mixture of isomers according to General Protocol C started from TClM isomers (586 mg, 839 µmol), TfOH (740 µL, 8.39 mmol, 10 equiv), and 3-chloroanisole (8.20 mL, 67.1 mmol, 80 equiv). The solid (556 mg, 796 µmol, 95%) obtained without trituration contained 108 mg (155 µmol, 19%) of **18** and 448 mg (641 µmol, 76%) of iTClM (**19**), according to ^{1}H NMR analysis.

1,3,5,7-Tetrakis(2-chloro-4-methoxyphenyl)adamantane (TClM, 15)

R_f = 0.11 (PE/CH_2Cl_2 1:1, v/v).

^{1}H NMR (400 MHz, $CDCl_3$): δ = 7.39 (d, *J* = 8.9 Hz, 4 H), 6.95 (d, *J* = 2.8 Hz, 4 H), 6.80 (dd, *J* = 8.9, 2.8 Hz, 4 H), 3.79 (s, 12 H), 2.66 (s, 12 H).

^{13}C NMR (101 MHz, $CDCl_3$): δ = 158.3, 137.4, 134.1, 128.7, 117.9, 112.6, 55.6, 41.6, 40.1.

HRMS (EI): *m*/*z* calcd for $C_{38}H_{36}Cl_4O_4$: 698.1339; found: 698.1334.

1-(4-Chloro-2-methoxyphenyl)-3,5,7-tris(2-chloro-4-methoxyphenyl)adamantane (16)

R_f = 0.21 (PE/CH_2Cl_2 7:3, v/v).

^{1}H NMR (300 MHz, CD_2Cl_2): δ = 7.42 (d, *J* = 8.9 Hz, 3 H), 7.29 (d, *J* = 8.8 Hz, 1 H), 6.96–6.91 (m, 5 H), 6.82 (dd, *J* = 9.0, 2.9 Hz, 3 H), 3.84 (s, 3 H), 3.78 (s, 9 H), 2.68 (d, *J* = 11.9 Hz, 3 H), 2.60 (d, *J* = 12.9 Hz, 3 H), 2.55 (s, 6 H).

^{13}C NMR (76 MHz, CD_2Cl_2): δ = 159.8, 158.6, 137.7, 136.0, 134.2, 132.9, 129.1, 127.9, 120.6, 118.1, 112.8, 112.5, 55.9, 55.7, 42.2, 41.8, 40.3, 39.9.

HRMS (EI): *m*/*z* calcd for $C_{38}H_{36}Cl_4O_4$: 698.1339; found: 698.1331.

1,3-Bis(2-chloro-4-methoxyphenyl)-5,7-bis(4-chloro-2-methoxyphenyl)adamantane (17)

R_f = 0.38 (PE/CH_2Cl_2 7:3, v/v).

^{1}H NMR (300 MHz, CD_2Cl_2): δ = 7.41 (d, *J* = 8.9 Hz, 2 H), 7.29 (d, *J* = 8.6 Hz, 2 H), 6.95–6.91 (m, 4 H), 6.81 (dd, *J* = 8.9, 2.8 Hz, 4 H), 3.84 (s, 6 H), 3.78 (s, 6 H), 2.63–2.42 (m, 12 H).

^{13}C NMR (76 MHz, CD_2Cl_2): δ = 159.5, 158.6, 138.0, 136.3, 134.3, 132.9, 129.1, 128.0, 120.6, 118.1, 112.7, 112.5, 55.9, 55.7, 42.3, 42.2, 42.0, 40.3, 39.8.

HRMS (EI): *m*/*z* calcd for $C_{38}H_{36}Cl_4O_4$: 698.1339; found: 698.1332.

1-(2-Chloro-4-methoxyphenyl)-3,5,7-tris(4-chloro-2-methoxyphenyl)adamantane (18)

R_f = 0.60 (PE/CH_2Cl_2 7:3, v/v).

^{1}H NMR (300 MHz, CD_2Cl_2): δ = 7.40 (d, *J* = 8.9 Hz, 1 H), 7.29 (d, *J* = 8.1 Hz, 3 H), 6.94–6.91 (m, 7 H), 6.81 (dd, *J* = 8.8, 2.8 Hz, 1 H), 3.83 (s, 9 H), 3.78 (s, 3 H), 2.54–2.47 (m, 9 H), 2.32 (d, *J* = 11.7 Hz).

^{13}C NMR (76 MHz, CD_2Cl_2): δ = 159.8, 158.5, 138.2, 136.5, 134.3, 132.8, 129.1, 128.1, 120.6, 118.1, 112.7, 112.5, 55.9, 55.7, 42.3, 42.1, 42.0, 40.2, 39.8.

HRMS (EI): *m*/*z* calcd for $C_{38}H_{36}Cl_4O_4$: 698.1339; found: 698.1330.

1,3,5,7-Tetrakis(4-chloro-2-methoxyphenyl)adamantane (iTClM, 19)

R_f = 0.83 (PE/CH_2Cl_2 1:1, v/v).

^{1}H NMR (400 MHz, $CDCl_3$): δ = 7.25 (d, signal under solvent peak), 6.92 (dd, *J* = 8.3, 2.0 Hz, 4 H), 6.87 (d, *J* = 8.3 Hz, 4 H), 3.82 (s, 12 H), 2.39 (s, 12 H).

^{13}C NMR (101 MHz, $CDCl_3$): δ = 159.5, 136.4, 132.7, 127.5, 120.5, 112.4, 55.5, 42.1, 39.4.

HRMS (ESI): *m*/*z* calcd for $C_{38}H_{36}Cl_4O_4$: 698.1339; found: 698.1334.

1,3,5,7-Tetrakis(2-fluoro-4-methoxyphenyl)adamantane (TFM, 21) and Regioisomers 22–24

General Protocol A with 3-fluoroanisole (4.6 mL, 40.0 mmol, 80 equiv), followed by column chromatography with PE/CH_2Cl_2 3.75:6.25 (v/v) as eluent yielded 36 mg (57 µmol, 11%) TFM (**21**), 65 mg (103 µmol, 21%) of **22**, 75 mg (119 µmol, 24%) of **23**, and 36 mg (57 µmol, 11%) of **24** as colorless solids.

Synthesis according to General Protocol B using TOA (250 mg, 1.25 mmol), tosylic acid (2.37 g, 12.5 mmol, 10 equiv), and 3-fluoroanisole (11.3 mL, 100 mmol, 80 equiv), followed by chromatography yielded 413 mg (653 µmol, 52%) of TFM (**21**) and 177 mg (653 µmol, 52%) of **22**.

A subsequent isomerization with the mixture of TFM isomers (961 mg, 1.52 mmol) according to General Protocol C was done with TfOH (1.3 mL, 14.7 mmol, 10 equiv) and 3-fluoroanisole (13.9 mL, 122 mmol, 80 equiv). Column chromatography without trituration yielded 832 mg (1.31 mmol, 87%) of TFM (**21**) and 63 mg (100 µmol, 7%) of **22**.

1,3,5,7-Tetrakis(2-fluoro-4-methoxyphenyl)adamantane (TFM, 21)

R_f = 0.12 (PE/CH_2Cl_2 1:1, v/v).

^{1}H NMR (400 MHz, $CDCl_3$): δ = 7.27 (t, *J* = 9.1 Hz, 4 H), 6.67 (dd, *J* = 8.7, 2.7 Hz, 4 H), 6.61 (dd, *J* = 14.6, 2.6 Hz, 4 H), 3.79 (s, 12 H), 2.36 (s, 12 H).

^{13}C NMR (101 MHz, $CDCl_3$): δ = 161.5 (d, $J_{C,F}$ = 248.5 Hz), 158.1 (d, $J_{C,F}$ = 11.7 Hz), 126.9 (d, $J_{C,F}$ = 10.7 Hz), 126.3 (d, $J_{C,F}$ = 7.7 Hz), 108.2 (d, $J_{C,F}$ = 2.4 Hz), 101.8 (d, $J_{C,F}$ = 28.1 Hz), 54.5, 42.6, 161.5 (d, $J_{C,F}$ = 248.5 Hz), 42.6, 37.2 (d, $J_{C,F}$ = 3.5 Hz).

^{19}F NMR (376 MHz, $CDCl_3$): δ = –107.5 (s, 4 F).

HRMS (EI): *m*/*z* calcd for $C_{38}H_{37}F_4O_4$: 633.2622; found: 633.2551.

1-(4-Fluoro-2-methoxyphenyl)-3,5,7-tris(2-fluoro-4-methoxyphenyl)adamantane (22)

R_f = 0.22 (PE/CH_2Cl_2 7:3, v/v).

^{1}H NMR (400 MHz, $CDCl_3$): δ = 7.28–7.24 (m, 4 H), 6.67–6.58 (m, 8 H), 3.81 (s, 3 H), 3.78 (s, 9 H), 2.40 (s, 6 H), 2.37 (d, *J* = 12. 0 Hz, 3 H), 2.29 (d, *J* = 12.0 Hz, 3 H).

^{13}C NMR (101 MHz, $CDCl_3$): δ = 162.5 (d, $J_{C,F}$ = 247.9 Hz), 162.2 (d, $J_{C,F}$ = 243.7 Hz), 159.7 (d, $J_{C,F}$ = 8.9 Hz), 159.1 (d, $J_{C,F}$ = 11.8 Hz), 132.6 (d, $J_{C,F}$ = 3.2 Hz), 128.3 (d, $J_{C,F}$ = 10.6 Hz), 127.4 (d, $J_{C,F}$ = 7.7 Hz), 127.3 (d, $J_{C,F}$ = 9.7 Hz), 109.2 (d, $J_{C,F}$ = 2.3 Hz), 106.3 (d, $J_{C,F}$ = 19.9 Hz) 102.9 (d, $J_{C,F}$ = 28.2 Hz), 99.9 (d, $J_{C,F}$ = 24.9 Hz), 55.5, 55.3, 43.8, 42.8 (d, $J_{C,F}$ = 3.4 Hz), 39.0, 38.3 (d, $J_{C,F}$ = 3.6 Hz).

^{19}F NMR (376 MHz, $CDCl_3$): δ = –107.5 (s, 3 F), –115.1 (s, 1 F).

HRMS (ESI): *m*/*z* calcd for $C_{38}H_{36}F_4O_4Na$: 655.2442; found: 655.2447.

1,3-Bis(2-fluoro-4-methoxyphenyl)-5,7-bis(4-fluoro-2-methoxyphenyl)adamantane (23)

R_f = 0.37 (PE/CH_2Cl_2 7:3, v/v).

^{1}H NMR (400 MHz, $CDCl_3$): δ = 7.29–7.24 (m, 4 H), 6.67–6.58 (m, 8 H), 3.81 (s, 6 H), 3.78 (s, 6 H), 2.44–2.31 (m, 12 H).

^{13}C NMR (101 MHz, $CDCl_3$): δ = 162.6 (d, $J_{C,F}$ = 247.5 Hz), 162.1 (d, $J_{C,F}$ = 243.6 Hz), 159.7 (d, $J_{C,F}$ = 9.0 Hz), 159.0 (d, $J_{C,F}$ = 11.7 Hz), 132.9 (d, $J_{C,F}$ = 3.5 Hz), 128.7 (d, $J_{C,F}$ = 10.4 Hz), 127.4 (d, $J_{C,F}$ = 8.0 Hz), 127.3 (d, $J_{C,F}$ = 9.5 Hz), 109.2 (d, $J_{C,F}$ = 2.4 Hz), 106.3 (d, $J_{C,F}$ = 19.9 Hz) 102.8 (d, $J_{C,F}$ = 28.2 Hz), 99.9 (d, $J_{C,F}$ = 25.0 Hz), 55.5, 55.3, 43.9, 43.0 (d, $J_{C,F}$ = 3.3 Hz), 42.2, 39.1, 38.3 (d, $J_{C,F}$ = 3.6 Hz).

^{19}F NMR (376 MHz, $CDCl_3$): δ = –107.5 (s, 2 F), –115.2 (s, 2 F).

HRMS (ESI): *m*/*z* calcd for $C_{38}H_{36}F_4O_4Na$: 655.2442; found: 655.2444.

1-(2-Fluoro-4-methoxyphenyl)-3,5,7-tris(4-fluoro-2-methoxyphenyl)adamantane (24)

R_f = 0.53 (PE/CH_2Cl_2 7:3, v/v).

^{1}H NMR (400 MHz, $CDCl_3$): δ = 7.29–7.24 (m, 4 H), 6.67–6.58 (m, 8 H), 3.81 (s, 9 H), 3.78 (s, 3 H), 2.42 (s, 6 H), 2.37 (s, 6 H).

^{13}C NMR (101 MHz, $CDCl_3$): δ = 162.6 (d, $J_{C,F}$ = 248.6 Hz), 162.1 (d, $J_{C,F}$ = 243.4 Hz), 159.7 (d, $J_{C,F}$ = 8.9 Hz), 159.0 (d, $J_{C,F}$ = 11.7 Hz), 133.3 (d, $J_{C,F}$ = 3.4 Hz), 129.0 (d, $J_{C,F}$ = 10.7 Hz), 127.5 (d, $J_{C,F}$ = 7.9 Hz), 127.4 (d, $J_{C,F}$ = 9.5 Hz), 109.1 (d, $J_{C,F}$ = 2.5 Hz), 106.2 (d, $J_{C,F}$ = 19.8 Hz) 102.8 (d, $J_{C,F}$ = 28.3 Hz), 99.8 (d, $J_{C,F}$ = 25.0 Hz), 55.5, 55.2, 43.1 (d, $J_{C,F}$ = 3.2 Hz), 42.3, 39.2, 38.3 (d, $J_{C,F}$ = 3.6 Hz).

^{19}F NMR (376 MHz, $CDCl_3$): δ = –107.5 (s, 1 F), –115.4 (s, 3 F).

HRMS (ESI): *m*/*z* calcd for $C_{38}H_{37}F_4O_4$: 633.2622; found: 633.2621.

Conflict of Interest

The authors declare no conflict of interest.

Funding Information

This work was supported by Deutsche Forschungsgemeinschaft (DFG), grant No. RI-1063/17-1, and the University of Stuttgart.

Acknowledgment

The authors would like to thank Felix Krupp, Stefanie Schiele, Thao Pham, and Ruben Pereira Rebelo for exploratory experiments and discussions.

Supporting Information

Supporting information for this article is available online at https://doi.org/10.1055/a-2097-0092.

References

(1) Tominaga, M.; Hyodo, T.; Maekawa, Y.; Kawahata, M.; Yamaguchi, K. *Chem. Eur. J.* **2020**, *26*, 5157.
(2) Tominaga, M.; Kunitomi, N.; Katagiri, K.; Itoh, T. *Org. Lett.* **2015**, *17*, 786.
(3) Tominaga, M.; Noda, A.; Ohara, K.; Yamaguchi, K.; Itoh, T. *Chem. Lett.* **2016**, *45*, 773.
(4) Hyodo, T.; Tominaga, M.; Yamaguchi, K. *CrystEngComm* **2021**, *23*, 1539.
(5) Nasrallah, H.; Hierso, J.-C. *Chem. Mater.* **2019**, *31*, 619.
(6) Li, X.; Guo, J.; Tong, R.; Topham, P. D.; Wang, J. *React. Funct. Polym.* **2018**, *130*, 126.
(7) Gowrisankar, S.; Bernhardt, B.; Becker, J.; Schreiner, P. R. *Eur. J. Org. Chem.* **2021**, e202101366.
(8) Müller, M. J.; Ziese, F.; Belz, J.; Hüppe, F.; Gowrisankar, S.; Bernhardt, B.; Schwan, S.; Mollenhauer, D.; Schreiner, P. R.; Volz, K.; Sanna, S.; Chatterjee, S. *Opt. Mater. Express* **2022**, *12*, 3517.
(9) Spasov, A. A.; Khamidova, T. V.; Bugaeva, L. I.; Morozov, I. S. *Pharm. Chem. J.* **2000**, *34*, 1.
(10) Wanka, L.; Iqbal, K.; Schreiner, P. R. *Chem. Rev.* **2013**, *113*, 3516.
(11) Merkle, R. C. *Nanotechnology* **2000**, *11*, 89.
(12) Tominaga, M.; Katagiri, K.; Azumaya, I. *Cryst. Growth Des.* **2009**, *9*, 3692.
(13) Tominaga, M.; Masu, H.; Azumaya, I. *Cryst. Growth Des.* **2011**, *11*, 542.
(14) Tominaga, M.; Takahashi, E.; Ukai, H.; Ohara, K.; Itoh, T.; Yamaguchi, K. *Org. Lett.* **2017**, *19*, 1508.
(15) Tominaga, M.; Yoneta, T.; Ohara, K.; Yamaguchi, K.; Itoh, T.; Minamoto, C.; Azumaya, I. *Org. Lett.* **2014**, *16*, 4622.
(16) Masu, H.; Tominaga, M.; Azumaya, I. *Cryst. Growth Des.* **2013**, *13*, 752.
(17) Tominaga, M.; Masu, H.; Azumaya, I. *CrystEngComm* **2011**, *13*, 5299.
(18) Tominaga, M.; Katagiri, K.; Azumaya, I. *CrystEngComm* **2010**, *12*, 1164.
(19) Stetter, H.; Schwarz, M.; Hirschhorn, A. *Angew. Chem.* **1959**, *71*, 429.
(20) Stetter, H.; Wulff, C. *Chem. Ber.* **1960**, *93*, 1366.
(21) Stetter, H.; Gärtner, J.; Tacke, P. *Chem. Ber.* **1965**, *98*, 3888.
(22) Stetter, H.; Krause, M. *Liebigs Ann. Chem.* **1968**, *717*, 60.
(23) Dolejšek, Z.; Hála, S.; Hanuš, V.; Landa, S. *Collect. Czech. Chem. Commun.* **1966**, *31*, 435.
(24) Tominaga, M.; Katagiri, K.; Azumaya, I. *CrystEngComm* **2010**, *12*, 1164.
(25) Schwenger, A.; Frey, W.; Richert, C. *Chem. Eur. J.* **2015**, *21*, 8781.
(26) Alexandre, P.-E.; Schwenger, A.; Frey, W.; Richert, C. *Chem. Eur. J.* **2017**, *23*, 9018.
(27) Krupp, F.; He, S.; Frey, W.; Richert, C. *Synlett* **2018**, *29*, 1707.
(28) Krupp, F.; Picher, M.-I.; Frey, W.; Plietker, B.; Richert, C. *Synlett* **2021**, *32*, 350.
(29) Rami, F.; Nowak, J.; Krupp, F.; Frey, W.; Richert, C. *Beilstein J. Org. Chem.* **2021**, *17*, 1476.
(30) Schwenger, A.; Frey, W.; Richert, C. *Angew. Chem. Int. Ed.* **2016**, *55*, 13706.
(31) Casco, M. E.; Krupp, F.; Grätz, S.; Schwenger, A.; Damakoudi, V.; Richert, C.; Frey, W.; Borchardt, L. *Adsorption* **2020**, *26*, 1323.
(32) Krupp, F.; Frey, W.; Richert, C. *Angew. Chem. Int. Ed.* **2020**, *59*, 15875.
(33) Fort, R. C.; von R. Schleyer, P. *Chem. Rev.* **1964**, *64*, 277.
(34) Shernyukov, A. V.; Salnikov, G. E.; Krasnov, V. I.; Genaev, A. M. *Org. Biomol. Chem.* **2022**, *20*, 8515.
(35) Fokin, A. A.; Shubina, T. E.; Gunchenko, P. A.; Isaev, S. D.; Yurchenko, A. G.; Schreiner, P. R. *J. Am. Chem. Soc.* **2002**, *124*, 10718.
(36) CCDC 2251141 (solvate-free form of iTBro) and 2251142 (iTBro with encapsulated CH_2Cl_2) contain the supplementary crystallographic data for this paper. The data can be obtained free of charge from The Cambridge Crystallographic Data Centre via www.ccdc.cam.ac.uk/structures.
(37) Richert, C.; Krupp, F. *Synlett* **2017**, *28*, 1763.
(38) Schwenger, A.; Gerlach, C.; Griesser, H.; Richert, C. *J. Org. Chem.* **2014**, *79*, 11558.
(39) Wrona-Piotrowicz, A.; Makal, A.; Zakrzewski, J. *J. Org. Chem.* **2020**, *85*, 11134.